Single Cytoplasmic Dynein Molecule Movements: Characterization and Comparison with Kinesin

Zhaohui Wang,* Shahid Khan,‡ and Michael P. Sheetz†*
*Department of Cell Biology, Duke University Medical Center, Durham, North Carolina, 27710, and ‡Department of Physiology and Biophysics, Albert Einstein College of Medicine, Bronx, New York 10461 USA

ABSTRACT Cytoplasmic dynein is a major microtubule motor for minus-end directed movements including retrograde axonal transport. To better understand the mechanism by which cytoplasmic dynein converts ATP energy into motility, we have analyzed the nanometer-level displacements of latex beads coated with low numbers of cytoplasmic dynein molecules. Cytoplasmic dynein-coated beads exhibited greater lateral movements among microtubule protofilaments (ave. 5.1 times/μm of displacement) compared with kinesin (ave. 0.9 times/μm). In addition, dynein moved rearward up to 100 nm over several hundred milliseconds, often in correlation with off-axis movements from one protofilament to another. We suggest that single molecules of cytoplasmic dynein move the beads because 1) there is a linear dependence of bead motility on dynein/bead ratio, 2) the binding of beads to microtubules studied by laser tweezers is best fit by a first-order Poisson, and 3) the run length histogram of dynein beads follows a first-order decay. At the cellular level, the greater disorder of cytoplasmic dynein movements may facilitate transport by decreasing the duration of collisions between kinesin and cytoplasmic dynein-powered vesicles.

INTRODUCTION

The transport of vesicular material, particularly in neurons, is powered by the microtubule motors, the most abundant of which are kinesin and cytoplasmic dynein. Kinesin and cytoplasmic dynein are also involved in a variety of other intracellular processes such as membrane traffic and mitosis (Schroer, 1992; Walker and Sheetz, 1993). Exactly how such motors convert the free energy of ATP hydrolysis into mechanical energy is not known. But in vitro assays of the movements of single kinesin molecules have provided important clues about the basic molecular mechanisms. Optical trapping and interferometry tracking of beads powered by single kinesin molecules have revealed 8-nm steps (Svoboda et al., 1993), in line with the observed distribution of kinesin-binding sites on microtubules (Harrison et al., 1993; Song and Mandelkow, 1993). Kinesin-powered bead movements, tracked with nanometer-level precision by video-enhanced differential interference contrast (DIC) microscopy, followed the path of single protofilaments (Gelles et al., 1988), a conclusion supported by more recent studies using zinc sheets (Kamimura and Mandelkow, 1992) and microtubules of different protofilament number (Ray et al., 1993). Movements of single cytoplasmic dynein molecules have not been analyzed to determine if they similarly show such order in movement at the single-molecule level.

Native "conventional" kinesin is an extended molecule about 80 nm in length. Its two amino-terminal globular heads, which are about 6 nm in diameter, contain ATP and microtubule binding sites and are capable of force generation (Hirokawa et al., 1989; Yang et al., 1990). In vitro motility of single-headed kinesin constructs has been demonstrated recently. Interestingly, beads driven by single-headed kinesins do not track single protofilaments but wander all over the microtubule (Berliner et al., 1995). This behavior, taken together with transient-state kinetic analysis of the kinesin ATPase activity (Gilbert et al., 1995), is consistent with models where the two kinesin heads walk hand over hand along the microtubule (Schnapp et al., 1990; Hackney, 1994). Cytoplasmic dynein is a multisubunit complex with a bouquet-like shape. From base to top, it is about 45 nm long. Cytoplasmic dynein also has two globular heads, which are about 12 nm in diameter, containing ATP and microtubule binding sites (Vallee et al., 1988; Neely et al., 1990). Dynein-based motility has classically been studied by analyzing sliding of axonemal microtubules (Sale and Satir, 1977). More recently, an in vitro motility assay has been developed to examine movements of microtubules over immobilized axonemal dyneins (Vale and Toyoshima, 1988; Vale et al., 1989). Preliminary in vitro motility studies with cytoplasmic dynein showed that it exhibited considerable off-axis movement similar to that of the single-headed kinesin (Gelles et al., 1989).

To study the mechanism of motor movement, it is necessary to monitor movements generated by single motor molecules. Single kinesin molecules can generate movements (Howard et al., 1989; Block et al., 1990), and motility generated by single or a low number of myosin molecules has also been produced (Finer et al., 1994; Ishijima et al., 1994). These observations have greatly increased the understanding of kinesin and myosin motility and force generation. However, the movements of dyneins have not been similarly characterized because it has been difficult to obtain movements with single dynein molecules.

Received for publication 19 April 1995 and in final form 28 July 1995.
Address reprint requests to Dr. Michael P. Sheetz, Department of Cell Biology, Duke University Medical Center, 388 Nanaline Duke Building, Research Drive, Durham, NC 27710. Tel.: 919-684-8091; Fax: 919-684-8592; E-mail: mike_sheetz@cellbio.duke.edu.

0006-3495/95/11/2011/00 $2.00

In this paper, we report the displacements of latex beads powered by single or a few cytoplasmic dynein molecules. We followed the displacements with a particle tracking method that has been used successfully in the past to follow movement of kinesin molecules bound to beads (Gelles et al., 1988). This nanometer-scale precision tracking method measures bead positions as the beads move along microtubules, by using cross-correlation analyses of video-enhanced DIC images and provides a sensitive measure of the path of motor movement.

MATERIALS AND METHODS

Materials

Taxol was purchased from Calbiochem (San Diego, CA). Ultrapure sucrose was from ICN Biomedicals, Inc. (Irvine, CA). Hexokinase, EDTA, and EGTA were purchased from Boehringer Mannheim GmbH (Germany). Fertilized chicken eggs were purchased from the veterinary school of North Carolina State University. Monoclonal antibodies against cytoplasmic dynein, 440.1 and 70.1, have been described previously (Steuer et al., 1990). SUK4 anti-kinesin heavy chain monoclonal antibody (Ingold et al., 1988) was a generous gift from Dr. Jon Scholey (UC-Davis). The polyclonal anti-tubulin antibody was from Amersham (Arlington Heights, IL). All other chemicals were purchased from Sigma (St. Louis, MO).

Microtubules were assembled by mixing phosphocellulose purified tubulin (3–14 mg/ml) (Williams and Lee, 1982) with GTP (1 mM) and taxol (20 μM) in PMEE′ (35 mM PIPES, 5 mM $MgSO_4$, 1 mM EGTA, 0.5 mM EDTA, pH 7.4) followed by incubation at 37°C for 15 min.

Preparation and characterization of motor coated beads

Chick cytoplasmic dynein and kinesin were purified from 11–12-day-old chicken embryo brains as previously described (Schroer et al., 1989), and the peak fractions were analyzed by SDS polyacrylamide gel electrophoresis to monitor purity. Kinesin from squid optical lobe was purified according to the method of Vale et al. (1985).

Motor coated beads were prepared by serial addition with mixing of 2 μl motility buffer (ATP, 6 mM dithiothreitol, 60 μg/ml α-casein in PMEE′), 2 μl of diluted kinesin or cytoplasmic dynein stock, and 6 μl of 143-nm-diameter latex beads (1/100 dilution of 2.5%, w/v stock) in a test tube. After incubation on ice for 2 min, 2 μl of 2.2 mg/ml α-casein was added to block further binding of motor molecules to the beads. The amount of motor molecules bound to the beads was estimated by banding the beads in a discontinuous sucrose gradient. The beads were banded at the 10–25% sucrose interface by centrifugation at 135,000 $\times$ g for 5 min and then carefully removed. The dynein in this bead fraction was measured by dot blotting with the Bio-Dot microfiltration apparatus (Bio-Rad Laboratories, Richmond, CA), using monoclonal antibodies against cytoplasmic dynein heavy chain (440.1) and intermediate chain (70.1) (Steuer et al., 1990). Serial dilution of a cytoplasmic dynein stock of known concentration was used as the standard concentration control in the dot blots. SUK4 monoclonal antibody was used to rule out kinesin contamination of the dynein-coated beads.

Protein concentrations were measured using Bio-Rad protein assay reagent (Bio-Rad, Hercules, CA). Gels and blots were densitometered using Deskscan II version 1.01 with HP ScanJet IIC (Hewlett Packard, Palo Alto, CA) and analyzed using NIH image 1.4 software.

Bead motility assay

Previous bead motility assays (Vale et al., 1985) were modified by standardization of the chamber design and the addition of α-casein (Schnapp et al., 1992). Chambers (~7 μl volume) were formed by sandwiching a coverslip (22 $\times$ 22 mm, no. 0) and the glass slide (25 $\times$ 75 mm) with two parallel lines of silicon stopcock grease (Dow Corning, Midland, MI) or strips of double sticky tape (3M Corp., St. Paul, MN). Coverslips cleaned with 14% nitric acid were rinsed with water and spun dry prior to use. Beads (190 nm diameter) (1/10,000 dilution of stock, 2.5%, w/v) were added to the chamber as markers. A 1:40 dilution of anti-tubulin antiserum was exchanged into the chamber. After incubation for 5 min, unbound antibody was washed away with excess PMEE′ (~40 μl). Microtubules were exchanged in 10 μl at ~0.1 mg/ml and incubated for 15 min at room temperature. The unbound microtubules were washed out with rinsing buffer (40 μl of 1 mM GTP, 1 mM dithiothreitol, 220 μg/ml α-casein, and 20 μM taxol in 0.5$\times$ PMEE′). Finally, motor-coated beads were introduced into the chamber.

Video and data analysis

Bead movements were observed by video-enhanced DIC microscopy and recorded in s-VHS format. Images were digitized and bead positions were determined in every video frame (i.e., 33 ms), using a cross-correlation calculation. The instrumentation and software used have been described previously (Gelles et al., 1988). The magnification was 42 nm/pixel and 34 nm/pixel for the x, y axes respectively.

It was necessary to determine microtubule orientation to resolve bead displacements parallel and perpendicular to the microtubule axis. Microtubule orientation was determined by linear, least-square fitting of the path of bead movement, as well as by connecting two points several microns apart on a video image of the microtubule with a straight line. The latter method was used, in particular, if the beads moved a short distance (<0.2 μm).

An off-axis jump was scored upon inspection of the perpendicular displacement versus time plots, when the following criteria were met: 1) there was a sudden discontinuity in the trace, linear movements at a small pitch with the microtubule axis were not scored; 2) the tracks before and after the jump represented two distinct clusters of positions, which spanned more than 60 video frames (2 s); 3) the displacement between the central axes of the two clusters of positions was larger than 20 nm, which is the minimum displacement of the bead center when the motor switches between protofilaments (see Fig. 1 *c*).

The concentration of motor proteins on the bead surface was expressed as the molar ratio of the protein to the beads. Using a molecular weight of 1,200,000 for cytoplasmic dynein and 350,000 for kinesin, their molarities were calculated. The molarity of the beads was also calculated from the mean diameter of 143 nm and volume of 1.53×10^{-15} ml. The density of the bead is 1.04 g/ml (manufacturer's manual), so the weight of each bead is $\sim 1.59 \times 10^{-15}$ g. Because the bead stock is 2.5% (w/v), there are $\sim 1.57 \times 10^{10}$ beads/μl of the stock. Thus by knowing how many microliters of the motor protein and bead stocks were added into the motility assay, the molar ratio of motor to bead was calculated.

To calibrate the motility of cytoplasmic dynein-bound beads at different motor concentrations, we scored motor coated beads that attached to microtubules either spontaneously or with a laser trap. The behavior of each bead attached to microtubules was put into one of three categories: moving, diffusing, or stationary. A bead was scored as stationary if it moved no more than 0.2 μm over the observation period of up to 3 min but no less than 2 s. 0.2 μm (i.e., 5 pixels) was the minimum displacement that could reliably be detected by inspection of the videotaped images. If a bead switched direction of movement multiple times over a short distance (e.g., a micron) in a random manner, it was scored as diffusing; otherwise, it was scored as moving.

To observe beads attaching to microtubules spontaneously, 10 video fields chosen randomly were analyzed for each concentration and each field was observed for 3 min. The numbers of beads attached to and moving on microtubules were counted. The total length of microtubules in each field was measured by a computer program developed in the lab. In the "laser trapping" experiment, beads were randomly grabbed by a laser trap (785 nm wavelength) from the solution and brought onto microtubules.

The laser used was an 890 titanium:sapphire laser pumped by an Innova 70 argon ion laser (Coherent, Inc., Palo Alto, CA). A bead was held at the microtubule for 1 to 2 s and then the laser trap was turned off and the behavior of the beads was recorded. To avoid grabbing the same bead again, two consecutively trapped beads were picked from areas at least several microns apart. However, if a bead did not attach to a microtubule during the first "trapping," an effort was made to grab it again. The power of the laser beam before entering the objective lens of the microscope was around 50 mW (we estimate that ~50% of the light is lost in the lens). During the entire process, a bead stayed in a laser trap for about 5 s.

RESULTS

Experimental system and noise analyses

We developed a bead motility assay to study the movement of cytoplasmic dynein. The movement of cytoplasmic dynein-bound beads on microtubules was analyzed by video-enhanced DIC microscopy. A diagram of the geometry of the experimental system shows a side view (Fig. 1 *a*), a cross section (shown as three possible bead positions; Fig. 1 *b*) and the projected positions of the bead centers when the motor is bound to all the possible binding sites on the microtubule lattice (assuming a single site on each tubulin dimer; Fig. 1 *c*).

The averaged bead positions were measured with nanometer precision every 33 ms by cross-correlation analysis (Gelles et al., 1988; Schnapp et al., 1988). A priori, three factors limit the precision of frame-to-frame determination of bead position: i) instrumentation error; ii) movements of the immobilized microtubules; iii) thermal motions of the beads resulting from flexibility of the bead-microtubule linkage. Instrumentation error was evaluated by adsorbing the 143-nm beads used for motor-coated bead preparations onto the coverslip, as well as the 190-nm marker beads. In these and other experiments, the positions of the 190-nm marker beads were always averaged over 21 frames (i.e., 0.7 s) to make a more accurate determination of their position. Frame-to-frame standard deviations in the distance between immobilized 143 nm–190 nm bead pairs were around 2 nm in both x and y axes (Table 1). Computation of the distance between bead pairs, as detailed previously (Gelles et al., 1988), was effective in correcting for drift resulting from mechanical instability over the longer periods (i.e., 100 s) used for tracking bead movements. The 21-frame averaged marker bead positions can still compensate for any slow stage drift, which was typically less than 5 nm/s. Throughout the paper, all bead positions are expressed relative to averaged marker bead positions for the same video frames. Positions of tubulin-antibody-coated beads had a 3 nm uncertainty. Therefore, relative movements of the antibody-immobilized microtubules were small or comparable to the mechanical stability of the microscope system. However, positions of motor-coated beads bound to microtubules in the absence of ATP had a frame-to-frame standard deviation of ~10 nm and ~30 nm in the parallel and perpendicular directions, respectively (Table 1). To ensure that this behavior represented beads tethered to the microtubule by motor molecules, only those beads that subsequently moved

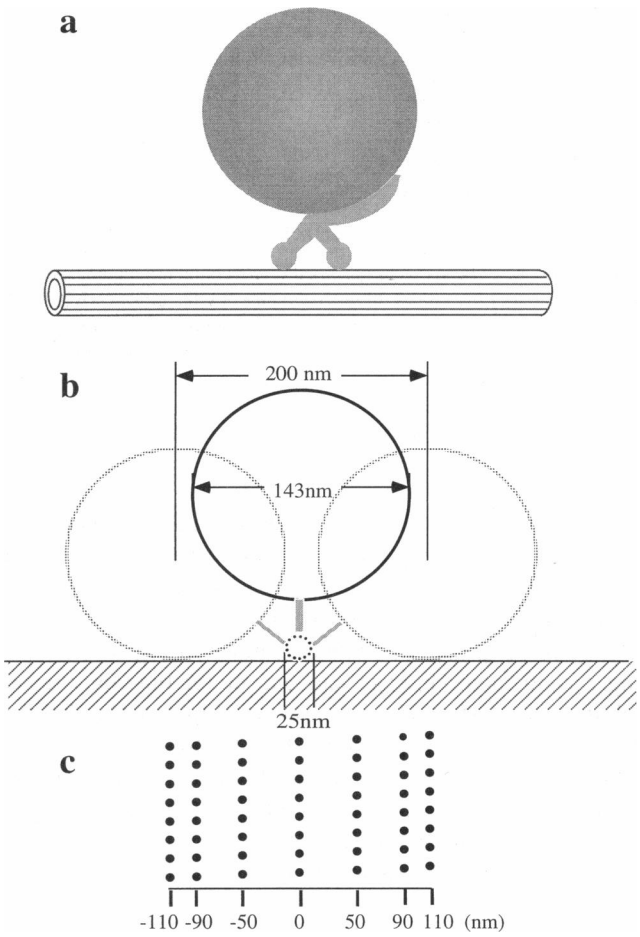

FIGURE 1 Schematic diagram of the bead-motor-microtubule system. (*a*) Side view of the system. (*b*) In this cross-section view of the system, the bead appears at three positions relative to the glass surface (the solid-line circle over the central protofilament and two dashed-line circles at either glass surface), the gray solid bars stand for the motor, and the small circle consisting of black dots stands for the microtubule. As marked, the bead is 143 nm in diameter and the microtubule is 25 nm in diameter. The center of the bead moves about 200 nm when it moves from one side of the microtubule to the other (dashed circles). (*c*) The black dots represent the projections of the center of the bead on the coverslip surface for all of the motor binding sites along the exposed half of the microtubule surface lattice. The dots were plotted by assuming 8 nm separation axially between sites (one tubulin dimer) and 32 nm for the length of the motor link between the bead and the microtubule. The scale bar shows the displacements of bead center when the motor moves from one protofilament to another.

or detached upon flowing in ATP were used for the analysis. Thus, flexibility in the motor linkage between bead and microtubule was the major factor limiting determination of bead position as previously documented for kinesin (Malik et al., 1994). The anisotropy of the thermal motions suggested that the stems of both cytoplasmic dynein and kinesin are 2- to 3-fold more flexible in the direction perpendicular to microtubule axis than in the parallel direction (Table 1), although somewhat greater movement in the perpendicular direction of the bead is expected from the geometry of the system (see Fig. 1 *b*).

Bead positions in the video field are two-dimensional, but the actual movements of motor-bound beads on microtu-

TABLE 1 Noise analyses

Bead Coating*	SD‡ of X coordinates (nm)	SD‡ of Y coordinates (nm)	No. of beads measured	Total no. of video frames analyzed§
Stationary beads on coverslip	2.0 ± 0.2	1.8 ± 0.6	5	4895
Antitubulin-coated beads on MTs	3.3 ± 1.7	2.6 ± 0.7	5	2400
Kinesin-coated beads on MTs	11.8 ± 7.2	21.7 ± 5.6	5	2900
Cytoplasmic dynein-coated beads on MTs	13.7 ± 5.7	31.3 ± 7.5	4	1920

*143-nm-diameter beads were adsorbed to coverslip surface nonspecifically or attached to microtubules by ways mentioned in the table. Their positions were measured at the rate of 30 video frames/s by the cross-correlation method. The positions of a 190 nm (diameter) reference bead were averaged over 21 video frames. The averaged positions were subtracted from the positions of the 143 nm beads in the same video frame to compensate for stage drift.
‡The standard deviation (SD) of the X and Y coordinates of the measured beads. In the cases of kinesin and cytoplasmic dynein, the X-axis is parallel to the microtubule axis, the Y-axis is perpendicular to the microtubule axis. The data are shown as the mean among the beads measured plus and minus the standard deviation of the measurements.
§The total number of the bead positions (or video frames) of all the beads measured.

bules are three-dimensional. What is actually measured by the method is the projection of bead positions on the focal plane; in this case it is the video field. The possible bead positions projected on the coverslip surface when the motor moves along the microtubule are shown in Fig. 1 *c*, assuming a rigid motor linkage and one motor binding site per tubulin dimer (Harrison et al., 1993; Song and Mandelkow, 1993). Each column of vertical dots illustrates motor movement along a microtubule protofilament. Seven protofilaments are shown because only half of the microtubule is accessible for motor binding. When the motor moves between adjacent protofilaments of a microtubule, the distances between the centroids of bead positions will range from 20 to 50 nm, depending upon the angle of the microtubule-bead axis relative to the coverslip surface. The largest lateral displacement when the bead moves from the glass on one side of the microtubule to the glass on the other would be 200 nm, given a 32-nm tether length (see below). In reality, the motor linkage is flexible and the bead will undergo thermal motions that will smear out the dots in Fig. 1*c*.

Pattern of movement of motor-bound beads

We have been able to observe motility of cytoplasmic dynein-coated beads at the average ratio of one dynein per bead. Two modifications of the assay helped us to obtain motility with single cytoplasmic dynein molecules. First, we decreased the final ionic strength in the assay (0.3 × PMEE′). We found that the number of cytoplasmic dynein-coated beads bound to microtubules (including moving beads) decreased as the ionic strength increased (data not shown). At about 1.3 × PMEE′, almost no beads bound to the microtubules. Second, the coverslip coating to immobilize the microtubules was modified. We used to air-dry the coverslips after addition of anti-tubulin antibodies to let the antibodies attach permanently. This process accumulated dust on the coverslip and created numerous air bubbles when solution was added again. Now we add the antibody solution into the flow chamber directly and let it incubate for 5 min, followed by a wash with PMEE′.

Cytoplasmic dynein-bound beads showed three kinds of behavior on microtubules: unidirectional movement, one-dimensional diffusion along the microtubule, and stationary binding. We determined the fraction of beads in each category as described in Materials and Methods. Within a given dynein preparation the fractions of actively motile or diffusing beads were not dependent on the number of dyneins per bead or the age of the preparation. With age, however, the total number of beads binding to the microtubules decreased dramatically. The fraction of actively moving beads was dependent on ATP and varied between different dynein preparations. When ATP was depleted, the fraction of stationary bound beads increased dramatically as both the actively motile and diffusing fractions decreased. Recent preparations where ATP was added before homogenization (the first step of the purification) and to the gradient had a higher fraction (40%) of actively motile beads than earlier preps without those components (15%). Only a small fraction of the beads showed a combination of the different behaviors. A study of the factors that modulate the diffusive behavior of motor-bound beads will be presented elsewhere.

Because of the large error due to the motor linkage vibration, we performed nanometer-scale position tracking of motor-coated beads at low ATP concentrations to enable temporal averaging of stationary positions on the microtubule lattice. Generally, we worked in the range of one to five cytoplasmic dynein molecules per bead. There were striking differences in the movement patterns of cytoplasmic dynein and kinesin. The typical path of cytoplasmic dynein-bound beads moving on microtubules is tortuous where positions cluster around separate parallel axes (Fig. 2 *a*). If we overlay the paths with the projected microtubule lattice in Fig. 1 *c*, the tortuosity of the paths can be explained as the motor moving on different protofilaments during active translocation. On the other hand, the movements of kinesin were mostly along the paths of single microtubule protofilaments (Fig. 2 *b*).

To analyze the movements in more detail, bead positions were decomposed into displacements parallel and perpendicular to the microtubule axis and plotted versus time (Fig. 3). In perpendicular displacements, cytoplasmic dy-

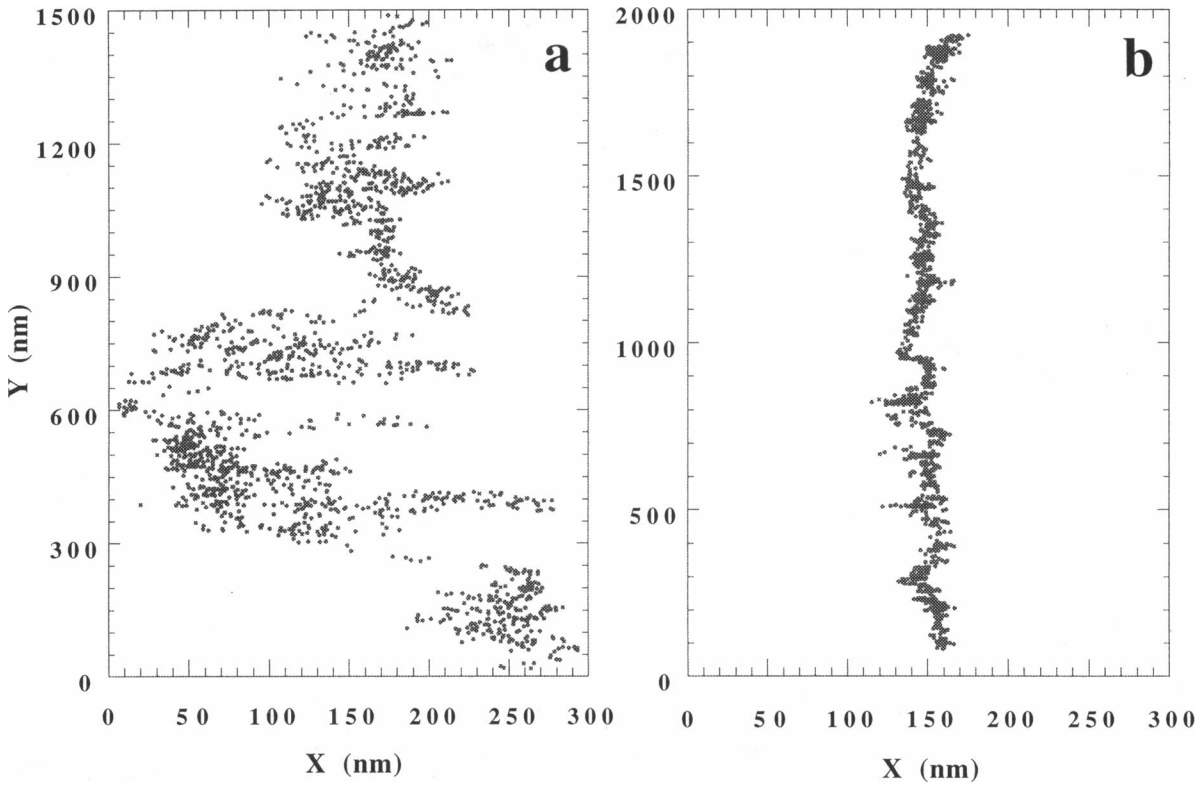

FIGURE 2 Paths of cytoplasmic dynein- and kinesin-coated beads moving along the microtubule surface lattice. The black dots represent bead positions measured every 33 ms. The microtubule axes are parallel to the *Y* axes. (*a*) Movement path of a cytoplasmic dynein-coated bead at 1 μM ATP with the ratio of ~0.8 motor per bead, in which the molecule moves over several protofilaments in 60 s. (*b*) Movement path of a kinesin-coated bead at 6 μM ATP with the ratio of ~1 motor per bead, in which the kinesin moves along a single protofilament for 60 s.

nein moved laterally over a range of about 200 nm and frequently switched from one axis to another, while kinesin followed a single axis with a path width of about 50 nm. The mean standard deviation of perpendicular displacements of cytoplasmic dynein is ~60 nm (n = 18) and that of kinesin is ~27 nm (n = 9). Similar analysis using root-mean-square displacements has shown that one-headed kinesin deviates more from a single axis than two-headed kinesin (Berliner et al., 1995). In parallel displacements there was a dramatic difference as well; cytoplasmic dynein frequently moved backward, whereas kinesin did not.

To further analyze whether cytoplasmic dynein was moving on different microtubule protofilaments, histograms were plotted with perpendicular displacements of cytoplasmic dynein- and kinesin-coated beads (Fig. 4). The bead position at the starting video frame was set to zero, and the relative perpendicular displacements in subsequent video frames to the starting frame were calculated and grouped with the bin size of 4 nm in the histograms. There are clearly several peaks in the histogram of cytoplasmic dynein movement (Fig. 4 *a*), as predicted if the motor were moving on several different protofilaments (see Fig. 1 *c*). The spread associated with each peak position was similar to the standard deviation of the stationary cytoplasmic dynein-bound beads (Table 1). Over 90% of the runs of cytoplasmic dynein-coated beads showed multiple peaks. However, it was not possible to distinguish which protofilament the motor was moving on before and after a switch in most cases. Because kinesin switches protofilaments much less frequently, a good match between the distribution of peaks and the microtubule lattice was occasionally discerned. For example, in Fig. 4 *c* the two peaks are about 40 nm apart, which is the distance between the second and third columns from either the left or right in Fig. 1 *c*. For kinesin-coated beads, about 60% of them exhibited single peak distribution (Fig. 4 *b*) with similar standard deviation as the stationary kinesin-bound bead, and about 40% showed more than one major peak in the histogram plots, although the number of peaks was usually less than that of cytoplasmic dynein-coated beads (Fig. 4 *c*). The diffusion envelope for bound cytoplasmic dynein or kinesin beads is clearly restricted, because on a totally flexible tether the bead would have a distribution with a width of at least 180 nm as opposed to the observed 50–70 nm. We find that the diffusion envelope does not change with movement for particles following a straight path. Furthermore, when the tracks along multiple paths are plotted as in Fig. 4, they can be fitted to a sum of Gaussians with the same 50–70-nm width. Because the standard deviation of stationary kinesin coated beads is

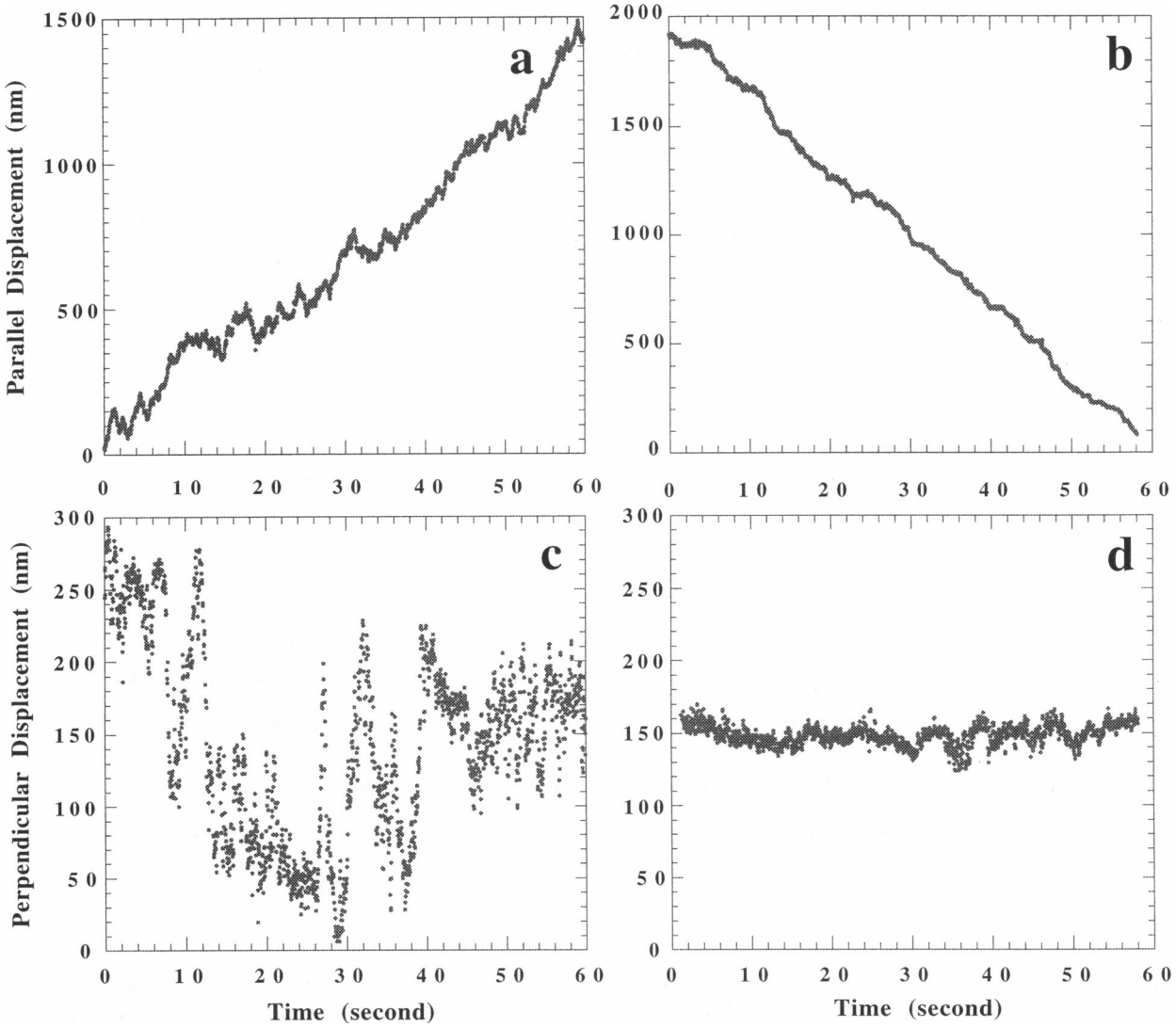

FIGURE 3 Positions of a cytoplasmic dynein-coated (*a* and *c*) and a kinesin-coated (*b* and *d*) bead parallel (*a* and *b*) and perpendicular (*c* and *d*) to the microtubule axes are plotted versus time (the same cytoplasmic dynein and kinesin coated beads as in Fig. 2). Note the larger rearward and off-axis movements of cytoplasmic dynein when compared with kinesin.

similar to that of cytoplasmic dynein-coated beads, the two motor arms have similar flexibility.

For quantitative comparison of the probability of switching protofilaments for cytoplasmic dynein and kinesin, we scored the frequency of off-axis jumps from the perpendicular versus time plots according to the procedure discussed in Materials and Methods. We measured the movements of more than 50 cytoplasmic dynein-bound beads. The average frequency of off-axis jump was calculated by dividing the sum of the off-axis jumps of the 50 beads by the sum of their displacements. On average, cytoplasmic dynein switches from one protofilament to another 5.1 times/μm of displacement. The frequency of off-axis movement varied from one run to another, and ranged from zero to as high as 60 switches/μm of displacement (Fig. 5). Kinesin only moved off-axis about 0.9 times/μm of displacement (n = 35), with many tracks showing no off-axis displacements (Fig. 5). The maximum off-axis jump frequency observed was 7 switches/μm. Thus, by several different criteria, cytoplasmic dynein switches between protofilaments more frequently than does kinesin.

The frequency of off-axis jumps for cytoplasmic dynein and kinesin did not vary with motor concentration ranging from 1 to 10 motors per bead (data not shown). The off-axis jump frequencies also did not vary with ATP concentration over the range of 1 to 100 μM (data not shown). This ruled out models where the increase in diffusive movements resulted from ATP-dependent transitions in motor conformation state. Both chick (n = 19) and squid (n = 16) kinesin were used in the motility assay, and they had similar movement patterns and off-axis movement frequencies. This indicates that the sixfold difference between the off-

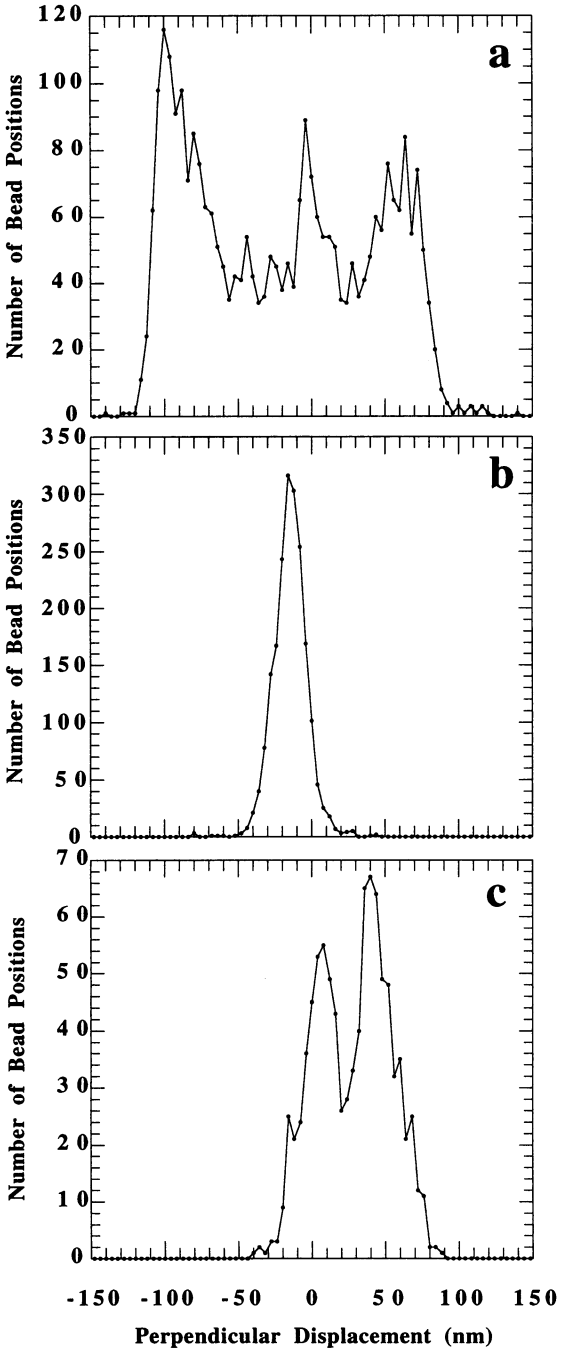

FIGURE 4 Histograms of the relative perpendicular displacements of cytoplasmic dynein- and kinesin-coated beads. The initial positions of the beads were arbitrarily set to zero, and the relative displacements of the subsequent positions from the initial position were calculated and grouped into bins 4 nm wide. A perpendicular displacement d is put into bin n if $4n \leq d < 4(n + 1)$, where $n = 0, \pm1, \pm2, \cdots, \pm100$. Any displacement with an absolute value larger than 400 nm was discarded as noise. The number of perpendicular displacements in each bin was scored and plotted. (*a*) The histogram of perpendicular displacements of a moving cytoplasmic dynein-coated bead shows several peaks. The cytoplasmic dynein/bead ratio was ~0.8 and the ATP concentration was 5 μM. The average velocity of the movement was 21 nm/s. (*b,c*) The histograms of perpendicular displacements of two moving kinesin-coated beads show single and double peaks, respectively. The kinesin/bead ratio was ~0.7. The ATP concentration was 1 μM and 25 μM, velocity was 12 nm/s and 80 nm/s for (*b*) and (*c*), respectively.

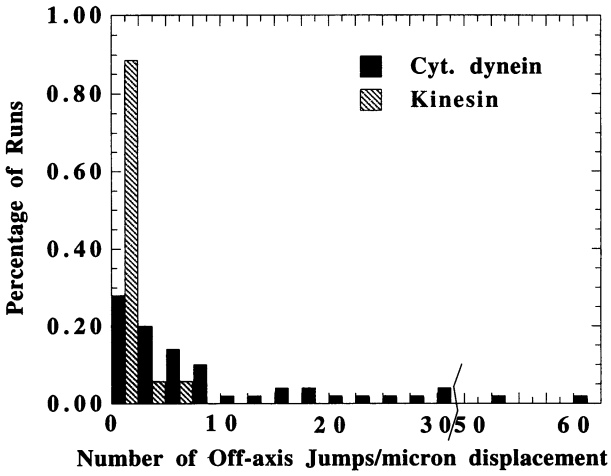

FIGURE 5 Histograms of the off-axis jumps of cytoplasmic (cyt.) dynein (dark bar) and kinesin (striped bar). The number of off-axis jumps was scored as mentioned in the Results section and calculated as the number per micron of parallel displacement for each run. The total number of runs examined was 50 for cytoplasmic dynein and 35 for kinesin. To make a comparison, the percentages of runs in each bin are shown. The bin width is 2.5, value x is grouped into bin n if $2.5\ n \leq x < 2.5, (n + 1)$, $n = 0, 1, \cdots$.

axis movement frequencies of kinesin and cytoplasmic dynein is not a species difference but rather is intrinsic to the two motors.

In displacements parallel to the microtubule axis, cytoplasmic dynein-bound beads often reversed direction for up to 100 nm (Fig. 3 *a*), while kinesin moved faithfully forward (Fig. 3 *b*). To determine whether the reverse movement of cytoplasmic dynein-bound beads was an artifact of bead vibration, we examined histogram plots of the parallel displacements between all pairs of bead positions separated by a half-second of moving and stationary beads. The interval of one half-second covers the duration of most of the rearward displacements. If the rearward displacement was simply due to thermal motion of the moving bead, the histogram distribution of rearward displacements should overlap that of stationary motor coated beads. The histogram of parallel displacement of moving cytoplasmic dynein-coated beads shows greater rearward movement than that of stationary dynein-coated beads as well as the greater forward movement as expected (Fig. 6 *a*). In contrast, the same analysis for kinesin showed that rearward displacements were within the thermal noise envelope obtained from stationary beads (Fig. 6 *b*). Although most detectable rearward displacements of cytoplasmic dynein ranged from 15 to 50 nm, consistent with the dimensions from electron microscopy of the tether length, displacements as large as 100 nm were observed. These displacements may arise from multiple rearward steps of the motor molecules.

To determine if the off-axis and reverse movements of cytoplasmic dynein were correlated, we inspected both the parallel and perpendicular displacements for some beads. As shown (Fig. 7), some rearward movements happened at the same time as off-axis jumps; some happened when no

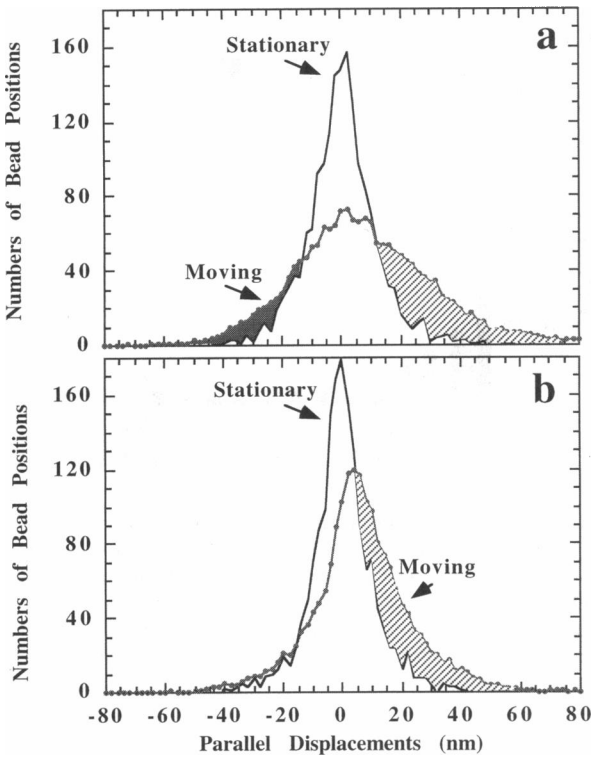

FIGURE 6 Parallel displacements of moving cytoplasmic dynein and kinesin-coated beads are compared with that of the stationary cytoplasmic dynein- and kinesin-coated beads on microtubules. Parallel displacements between any two positions of a bead separated by a half-second (15 video frames) were calculated and grouped into bins 2 nm wide. The displacements were put into bins according to the same rule as in Fig. 4. The number of bead pairs whose parallel separation fell into each bin was scored and plotted on the *Y*-axis. The stationary bead histograms are the sum of the individual histograms of four stationary beads for both cytoplasmic dynein and kinesin. Each stationary bead measurement was over 480 video frames. The moving bead histograms are the average of seven beads with 1920 video frames each for both motors. The averaging was done by summing the seven histograms and then dividing the sum by 7. (*a*) Histograms of moving (beaded string) and stationary (solid curve) cytoplasmic dynein coated beads. The cytoplasmic dynein/bead ratio is ~0.8. The velocity of the moving beads is from 9 to 23 nm/s at 0.5–1 μM ATP. (*b*) Histograms of moving (beaded string) and stationary (solid curve) kinesin-coated beads. The kinesin/bead ratio is ~1. The velocity is 5–13 nm/s at 1–5 μM ATP. The stippled areas in (*a*) and (*b*) show net forward movement relative to the stationary beads. The dark area in (*a*) shows rearward movement relative to the stationary beads.

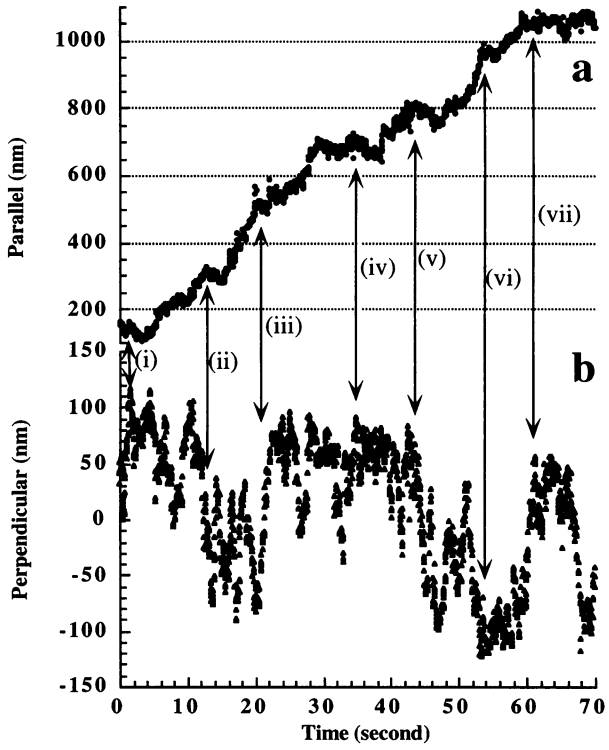

FIGURE 7 Comparison of the coincidence of rearward movement and off-axis jumps of cytoplasmic dynein coated beads. (*a*) Parallel displacement vs. time. (*b*) Perpendicular displacement vs. time of the same bead. The cytoplasmic dynein/bead ratio was ~0.8 and the ATP concentration was 0.75 μM. The two-headed arrows point to rearward movement in the parallel displacement and/or off-axis jump in the perpendicular displacement. Arrows i and iv point to two rearward movements of 50 nm and 70 nm, respectively, which occurred when no off-axis jump larger than 30 nm occurs. Arrows ii, iii, and vi point to rearward movements that happened right before or after off-axis jumps larger than 50 nm. Arrow v points to a rearward movement happened at the same time as an off-axis jump. Arrow vii points to an off-axis jump when no rearward movement was observed in the parallel displacement.

jumps between protofilaments occurred and vice versa; and some rearward movements occurred right before or after off-axis jumps. For seven paths examined (a total of 585 seconds of run time), 56% of the reverse movements were accompanied by off-axis jumps at the same time (a total of 81 reverse movements). The high correlation between reverse and off-axis movements suggests that some reverse movements were probably consequences of off-axis movements or vice versa. Still, a substantial fraction of rearward and off-axis movements were independent of each other.

To check if the reverse movement of cytoplasmic dynein was due to kinesin contamination, a Western blot analysis with the SUK4 monoclonal antibody against kinesin heavy chain was performed. No kinesin contamination was observed. Another possibility to explain reversals was movement on adjacent antiparallel microtubules. However, such examples would be expected to be rare, whereas, in contrast, reverse movements were observed in almost every run. Furthermore, the extent of reverse displacements was typically shorter than 100 nm. Consequently, rearward movement appeared to be a feature of pure cytoplasmic dynein.

There are currently no estimates of the length of the motor arm linking beads and microtubules in solution. Several electron microscope analyses showed that the motor arms are 20–30 nm long in vesicles attached to microtubules (Hirokawa et al., 1989; Miller and Lasek, 1985; Dailey and Bridgman, 1991). The length of the dynein tether connecting beads and microtubules was estimated as follows. Of 41 movements, 16 (37%) had a path width of 190–210 nm (measured between the outmost peaks of the position histograms (Fig. 4); the rest had a path width of 60–180 nm (with several showing an incomplete sampling of the microtubule surface). Assuming that 1) the average

maximum width of the path is 200 nm, 2) the dynein arm is a rigid rod, and 3) the arm always points to the center of the bead, we calculated its length based on the sketch in Fig. 1 *b* using the equation $c^2 = a^2 + b^2$, where c = 12.5 nm (radius of the microtubule) + motor tether length + 71.5 nm (radius of the bead), a = 100 nm (half of the maximum path width), b = 71.5 nm − 12.5 nm = 59 nm. The calculated length is 32 nm, which is consistent with available structural data.

Dependence of bead motility on cytoplasmic dynein concentration

To determine whether single cytoplasmic dynein molecules were capable of moving beads, two different criteria were examined. In the first case, we measured the increase in the number of motile beads as a function of the motor/bead ratio analogous to the approach used for kinesin by Howard et al. (1989). The second approach utilized a laser trap to bring beads down onto microtubules, and the fraction of beads that bound and/or moved was determined as a function of the motor/bead ratio. This approach has been used for kinesin by Block et al. (1990).

The cytoplasmic dynein used in the motility assay was the relatively pure sucrose gradient fraction. Cytoplasmic dynein accounted for about 80% of the protein in the fraction as determined by Coomassie blue staining. Protein contaminants include the tubulins and actin but not kinesin. In determining the molar ratio of cytoplasmic dynein to beads in the assay, the fraction of cytoplasmic dynein that bound to the beads during the 2-min incubation was measured by a quantitative dot blot with antibodies (see Materials and Methods). Seventy to ninety percent of the cytoplasmic dynein bound to the beads during the incubation, and the percentage of the cytoplasmic dynein bound increased with greater dilution. Monomeric fractions of cytoplasmic dynein (20S) were used within 24 h to avoid aggregation.

We measured the fraction of moving beads by scoring the number of beads that bound and moved on microtubules for 3 min in each of ten fields at different molar ratios of cytoplasmic dynein to beads. There was a linear increase in the number of beads per micron binding to and moving on microtubules when plotted against the ratio of motor to beads (Fig. 8). Assuming a maximum dimension of 45 × 45 nm^2 for cytoplasmic dynein when it lies flat, at least 26 molecules may be adsorbed onto 143-nm beads. Thus we are not saturating the bead surface and are likely to be within the linear region of the Langmuir isotherm of adsorption. The linearity suggests that cytoplasmic dynein molecules function independently in binding to and moving on microtubules. However, we also noticed that only a small fraction (~15%) of the beads that were bound to microtubules subsequently moved. This could be due to denaturation of cytoplasmic dynein during preparation or adsorption to the bead surface.

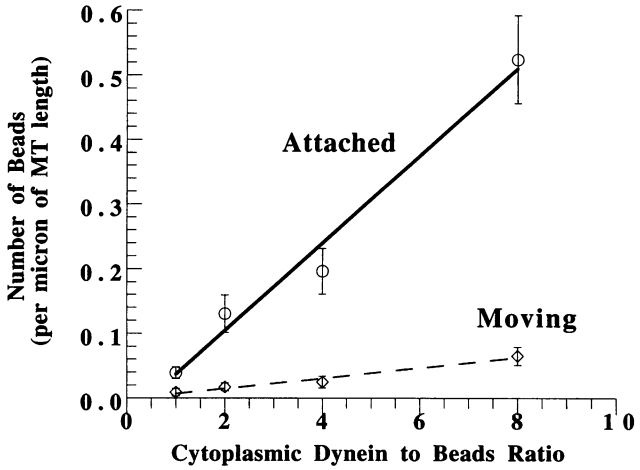

FIGURE 8 Linear dependence of bead binding to and moving on microtubules on the concentration of cytoplasmic dynein on the bead surface. The cytoplasmic dynein/bead ratio is calculated by dividing the number of bound cytoplasmic dynein molecules by the number of beads. The number of beads that moved on and attached to microtubules was counted for 3 min per field, and then calculated as the number per micron of microtubule length. Each data point shown here is the average of 10 fields. The number of beads that attached and moved per micron of microtubules increased linearly with the molar ratio of cytoplasmic dynein to bead (the solid and dashed lines are the linear fitting of the data).

To further determine if a fraction of the bound cytoplasmic dynein was inactive, we used the laser tweezers to bring the beads to the microtubule surface. About 100 beads, at various cytoplasmic dynein/bead ratios, were randomly "grabbed" from the solution and brought onto the microtubules with the laser tweezers. Some beads bound to the microtubules and a fraction subsequently moved. The percentage of beads that bound to microtubules (Fig. 9 *a*, triangles), which included all moving, diffusing, or stationary beads, was much lower than the percentage of beads with at least one motor estimated from Poisson statistics. However, this does not imply that more than one dynein molecule is required for motility, because, as noted above, a large fraction of the cytoplasmic dynein molecules appear inactive.

We modeled the behavior of motor-bound beads using Poisson statistics for the cases of movement by one, two, or three motor molecules. If multiple motor molecules are required for motility, two or more cytoplasmic dynein molecules need to contact each other. A minimal quantitative model for estimation of the concentration dependence of the motile fraction requires an additional space parameter to reflect the proximity of the motor molecules on the bead. From top to bottom, an extended cytoplasmic dynein molecule is 45 nm long, and two such molecules can reach 90 nm. Therefore, two cooperative cytoplasmic dynein molecules need to be within a circle of radius 90 nm. The surface area of a bead with a diameter of 143 nm can be roughly divided into three such circled areas. Consequently, a factor of one-third was used to compensate for the necessity of motor-motor contact in models requiring more than one

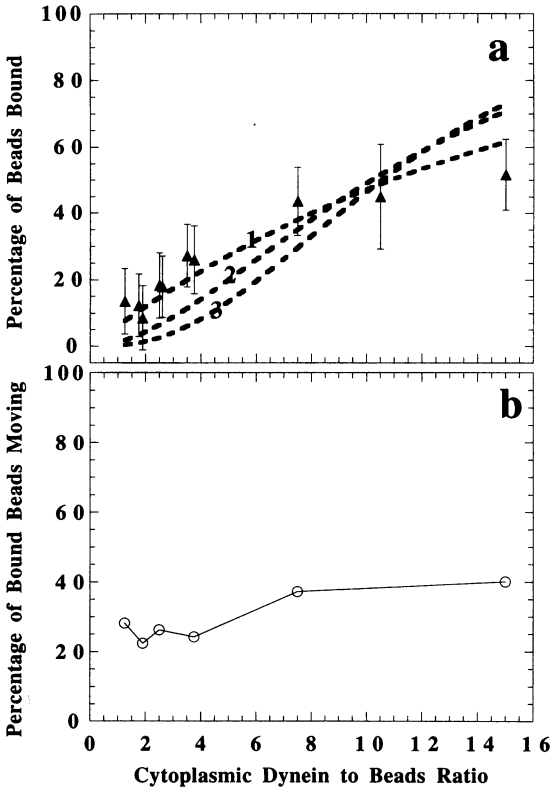

FIGURE 9 Laser tweezers sampling of bead binding to microtubules as a function of cytoplasmic dynein/bead ratio. Cytoplasmic dynein-coated beads in solution were "grabbed" randomly by a "laser trap" and placed onto a microtubule for ~2 s. At each ratio, about 100 beads were sampled and the percentage that bound to and moved on the microtubules was calculated. Cytoplasmic dynein/bead ratio was calculated the same way as in Fig. 8. (*a*) The triangles represent the percentages of cytoplasmic dynein-bound beads that bound to microtubules at different cytoplasmic dynein/bead ratios. The dashed lines marked 1, 2, and 3 are the expected percentage if only a single cytoplasmic dynein, or two, or three are required for movement, respectively. The calculation of the expected percentages was based on Poisson distribution and elaborated in the Results section. The error bars were calculated according to the sample size n ($1/\sqrt{n}$). (*b*) The percentage of bound beads that subsequently moved on the microtubules (open circles) does not change very much as the cytoplasmic dynein/bead ratio increases.

motor. The concentration dependence was estimated by using Poisson statistics, modified to incorporate this division of the bead surface area.

The data fit best (0.93 correlation coefficient) with the single motor model (Fig. 9 *a*) assuming that 6% of the motor population was active. The fitting function used was $f(X) = 100 * (1 - e^{-aX})$, where $f(X)$ is the motile fraction, X is the cytoplasmic dynein/bead ratio, and a is the fraction of active motors (calculated from the best fit of the data). For the two-motor model, the Poisson function is $f(X) = 100 * (1 - e^{-aX/3} - aX/3 * e^{-aX/3})$. The best fit (0.58 correlation coefficient) assumes 50% of the motor population was active. The fitting function of the three-motor model is $f(X) = 100 * (1 - e^{-aX/3} - aX/3 * e^{-aX/3} - (aX/3)^2/2 * e^{-aX/3})$. The best fit (0.35 correlation coefficient) assumes 76% of the motor population to be active. It is apparent that the data fit best with the single-motor model. As the number of motors required to generate movement increases, the data fit poorer and poorer, especially at a ratio of cytoplasmic dynein to beads of less than 5. With a sample size of 10 and 95% confidence, the correlation coefficient needs to be greater than 0.632 to have true correlation. Therefore, the single motor model fitting is truly correlative but the two-motor and three-motor model fittings are not. Thus, our data are mostly readily compatible with the postulate that single cytoplasmic dynein molecules can drive movement, but only a fraction of the cytoplasmic dynein preparation was active.

Cytoplasmic dynein may be inactivated during protein preparation or laser trapping. Trapping of moving cytoplasmic dynein-coated beads with a power similar to that used for applying the beads to the microtubule for 5 s stopped the beads (n = 14). Upon releasing of the trap, ~60% of the beads resumed movement right away, and more than 90% resumed movement within 2 min. The low active fraction cannot be explained by laser damage. The fraction of bound beads that move does not change significantly as the ratio of cytoplasmic dynein to beads increases (Fig. 9 *b*), which again suggests that no cooperation is needed for movement.

Another feature of single motor movement is that the beads should dissociate from the microtubule after a short run length that reflects the probability of detachment (Block et al., 1990). The exponential distribution of run lengths (Fig. 10) is consistent with movement generated by single motor molecules that have a constant probability of detaching at every step. The run lengths of bead movements free of diffusion or pauses were used to plot the histogram. Excluded were more complex movements that may incorporate transitions between inactive and active cytoplasmic dynein conformational states. The average run length is 0.89 μm. In Fig. 10, data were pooled from beads with cytoplas-

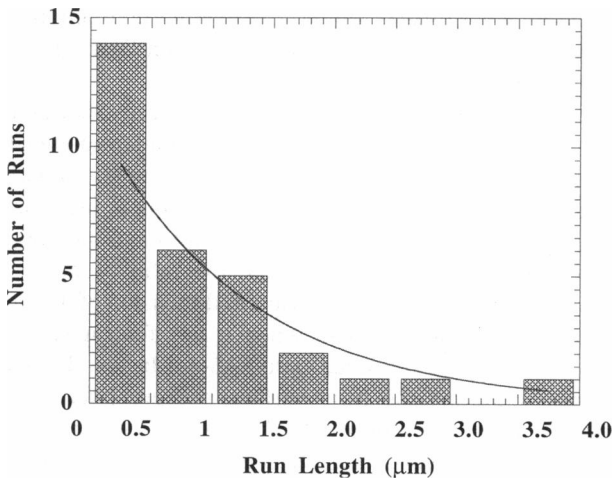

FIGURE 10 The distribution of run length of cytoplasmic dynein-coated beads placed on microtubules with laser tweezers. The run lengths were grouped into 0.5-μm-wide bins as in Fig. 5. The solid curve is a single exponential fitting of the data, which were fit according to the mean run length in each bin. The runs were pooled from moving bead populations at cytoplasmic dynein/bead ratio of 1 to 15 with 1 mM ATP.

mic dynein to bead ratios from 1 to 15 per bead. If only 6% of the cytoplasmic dynein molecules are active, there will be, on average, 0.06 to 0.9 active cytoplasmic dynein molecules per bead at these ratios. The single exponential nature of the run lengths is consistent with the hypothesis that a single motor drives the movement.

The above experiments indicate that single cytoplasmic dynein molecules are capable of moving along microtubules. They also showed that dynein binding to microtubules in the presence of ATP does not always result in movement.

DISCUSSION

In these studies we have used anionic latex beads to follow motor movements along microtubules. Even though there might be a brief temporal and spatial lag between movements of beads and that of the motors, the beads faithfully reflect motor movements on relatively long temporal and spatial scales. We can detect lateral motor movements between microtubule protofilaments readily, but displacements between individual tubulin subunits are at the limit of the method. The limitations of tracking objects by video-enhanced DIC microscopy have been treated elsewhere (Schnapp et al., 1988). For the present experiments the limitations are about 4 nm/frame for 143-nm beads attached to the glass surface and 60 ms between totally independent events because of the interlaced nature of the video frames.

We found that actively moving, single cytoplasmic dynein molecules exhibit five- to six-fold more random movements perpendicular to the microtubule axis and many more reverse movements than kinesin. The probability of moving off-axis was constant per displacement step and was not dependent on stepping frequency, because there was no dependence of the number of off-axis movements per micron of displacement on velocity. Although the off-axis jumps could occur during one step of active movement of the motors, the long time required for off-axis movement makes it look like several displacements of the bead are involved. We postulate that several steps are taken when the motor moves laterally, from one side of the microtubule to the other. Several factors that could affect the movement behavior were considered: 1) an unfolding of the molecule, 2) switching between multiple motors, 3) microtubule lattice defects, and 4) the release of one head from the microtubule lattice. The off-axis and rearward movements could result from changes in the motor tether length as the result of unfolding of the motor. We have discounted that possibility because tether length changes should give isotropic movements, whereas the motor movements are distinctly anisotropic. In the case of off-axis movements, each off-axis jump involved rapid displacements over several video frames; whereas before, during, and after the jump, the instantaneous thermal noise was unchanged.

We do not think that the differences in the movement patterns of cytoplasmic dynein and kinesin were due to differences in motor number per bead. First, the frequency of off-axis jumps does not vary significantly with the motor/bead ratio for either kinesin or cytoplasmic dynein, as observed in this study and previously (Gelles et al., 1988, 1989). Second, under our assay conditions (on average, 1 to 5 cytoplasmic dynein molecules per bead, and we estimate 0.06 to 0.3 active motors per bead), the probability of two active cytoplasmic dynein molecules contacting each other on the bead surface to act cooperatively is negligible. Third, we have demonstrated that single cytoplasmic dynein molecules can move on microtubules using approaches similar to those used for kinesin (Howard et al., 1989; Block et al., 1990).

The variation in the number of off-axis movements per micron was very large, which suggests that either there was significant variability in the motors on the beads or in the microtubule structure. Similar lateral movements were observed with kinesin as well, but the frequency was about sixfold lower, which suggests that the motor and not the microtubule is the primary determinant of off-axis movement. Previous studies with multiple kinesins suggested that it followed a single protofilament (Gelles et al., 1988), and other studies with different microtubule structures showed that movements of kinesin molecules followed single protofilaments (Kamimura and Mandelkow, 1992; Ray et al., 1993).

We believe that the off-axis and rearward movements of cytoplasmic dynein result from Brownian motion of the motor head involved in active movement. During movement of two-headed cytoplasmic dynein, one head must naturally release from the microtubule. When that head is released, it can diffuse to other protofilaments as little as 4 nm away or in a reverse direction to bind to other tubulin dimers. Because of their temporal correlation, the off-axis movements may be related to the rearward displacements and both could arise from a single diffusive movement of a head both off-axis and rearward. However, available data do not establish a clear-cut correlation between these two types of movement. The rearward movement could represent events where the segmental flexibility within the molecule allows the free head to bind to a rearward site. For forward movement to occur, such events have to be unfavorable and they may be correlated with the deformation of the molecule on the anionic bead surface.

It is interesting that kinesin is capable of random lateral movements particularly as a single headed molecule, even though it may prefer to follow a protofilament as a dimeric molecule (Berliner et al., 1995). Uncoupling of the heads in that case leads to off-axis movements, implying that the cytoplasmic dynein heads may normally be less coupled than kinesin. Kinesin made fewer rearward displacements under the same assay conditions, suggesting that it has less segmental flexibility between the heads. Recently Svoboda et al. (1994) reported that kinesin sometimes slips backward 8 nm under high load, which is considerably shorter than the rearward displacements of cytoplasmic dynein. Structural analyses of the motors have revealed that kinesin has

smaller heads that are more closely spaced than cytoplasmic dynein, which is consistent with the greater flexibility of the cytoplasmic dynein head movements (Vallee et al., 1988; Hirokawa et al., 1989; Neely et al., 1990). Therefore, a single mechanism of movement for these two motors is still consistent with the different displacement patterns. In both cases a motor head is always bound when the other head searches for the next binding site along the microtubule. Theoretically, the detached head of any motor has the chance to diffuse over to another protofilament and bind to the next site on that path. But different motors have different structural restrictions and their arms may not be equally flexible.

The ability of single cytoplasmic dynein molecules to undergo precessive movement along a microtubule suggests that the ATPase cycle is altered from that of axonemal dynein or skeletal myosin. Both of those motors are in a low affinity state for a major portion of the ATPase cycle that would result in bead detachment from the microtubule (Johnson, 1985). Exactly how the ATPase cycle is modified to allow precessive motion is unclear. There are several possible points in the ATPase cycle that could be altered to keep the motor from releasing during successive steps. One clear mechanism is to link the motility of the two heads by making release of the first head dependent upon the force produced by the second head. Clearly, some of the myosins that drive vesicle movement appear to have an altered ATPase cycle, which enables them to be precessive (Kuznetsov et al., 1992). Thus, we suggest that the cytoplasmic dyneins and some myosins have a modified ATPase cycle that lengthens the fraction of time the head spends in a high-affinity state bound to the substrate filament.

The difference in the movement patterns of cytoplasmic dynein and kinesin may have physiological significance as well. During vesicle transport in vivo, when two vesicles are moving in opposite directions on the same microtubule, they can collide on the same protofilament of the microtubule. Cytoplasmic dynein's greater off-axis movements would facilitate vesicle escape after the collisions. In terms of mechanisms of motor movement, the greater off-axis and rearward movements imply that the mechanism of movement can accommodate considerable disorder and yet allow forward movement.

Special thanks to Dr. Mike Reedy, Dr. Harold Erickson, and Dr. Andreas Bremer for their careful reading of the manuscripts and helpful comments.

This work was supported by grants from the National Institutes of Health to M.P.S. (NS23345) and S.K. (GM36936).

REFERENCES

Berliner, E., E. C. Young, K. Anderson, H. K. Mahtani, and J. Gelles. 1995. Failure of a single-headed kinesin to track parallel to microtubule protofilaments. *Nature.* 373:718–721.

Block, S. M., L. S. Goldstein, and B. J. Schnapp. 1990. Bead movement by single kinesin molecules studied with optical tweezers. *Nature.* 348: 348–352.

Dailey, M. E., and P. C. Bridgman. 1991. Structure and organization of membrane organelles along distal microtubule segments in growth cones. *J. Neurosci. Res.* 30:242–258.

Finer, J. T., R. M. Simmons, and J. A. Spudich. 1994. Single myosin molecule mechanics: piconewton forces and nanometre steps. *Nature.* 368:113–119.

Gelles, J., B. J. Schnapp, and M. P. Sheetz. 1988. Tracking kinesin-driven movements with nanometre-scale precision. *Nature.* 331:450–453.

Gelles, J., E. Steuer, B. J. Schnapp, and M. P. Sheetz. 1989. Movement of cytoplasmic dynein on the microtubule lattice. *J. Cell Biol.* 109:157a.

Gilbert, S. P., M. R. Webb, M. Brune, and K. A. Johnson. 1995. Pathway of processive ATP hydrolysis by kinesin. *Nature.* 373:671–676.

Hackney, D. D. 1994. Evidence for alternating head catalysis by kinesin during microtubule-stimulated ATP hydrolysis. *Proc. Natl. Acad. Sci. USA.* 91:6865–6869.

Harrison, B. C., R. S. Marchese, S. P. Gilbert, N. Cheng, A. C. Steven, and K. A. Johnson. 1993. Decoration of the microtubule surface by one kinesin head per tubulin heterodimer. *Nature.* 362:73–75.

Hirokawa, N., K. K. Pfister, H. Yorifuji, M. C. Wagner, S. T. Brady, and G. S. Bloom. 1989. Submolecular domains of bovine brain kinesin identified by electron microscopy and monoclonal antibody decoration. *Cell.* 56:867–878.

Howard, J., A. J. Hudspeth, and R. D. Vale. 1989. Movement of microtubules by single kinesin molecules. *Nature.* 342:154–158.

Ingold, A. L., S. A. Cohn, and J. M. Scholey. 1988. Inhibition of kinesin-driven microtubule motility by monoclonal antibodies to kinesin heavy chains. *J. Cell Biol.* 107:2857–2667.

Ishijima, A., Y. Harada, H. Kojima, T. Funatsu, H. Higuchi, and T. Yanagida. 1994. Single-molecule analysis of the actomyosin motor using nano-manipulation. *Biochem. Biophys. Res. Commun.* 199: 1057–1063.

Johnson, K. A. 1983. The pathway of ATP hydrolysis by dynein. Kinetics of a presteady state phosphate burst. *J. Biol. Chem.* 258: 13825–13832.

Johnson, K. A. 1985. Pathway of the microtubule-dynein ATPase and the structure of dynein: a comparison with actomyosin. *Annu. Rev. Biophys. Biophys. Chem.* 14:161–188.

Kamimura, S., and E. Mandelkow. 1992. Tubulin protofilaments and kinesin-dependent motility. *J. Cell Biol.* 118:865–875.

Kuznetsov, S. A., G. M. Langford, D. G. Weiss. 1992. Actin-dependent organelle movement in squid axoplasm. *Nature.* 356:722–725.

Malik, F., D. Brillinger, and R. D. Vale. 1994. High-resolution tracking of microtubule motility driven by a single kinesin motor. *Proc. Natl. Acad. Sci. USA.* 91:4584–4588.

Miller, R. H., and R. J. Lasek. 1985. Cross-bridges mediate anterograde and retrograde vesicle transport along microtubules in squid axoplasm. *J. Cell Biol.* 101:2181–2193.

Neely, M. D., H. P. Erickson, and K. Boekelheide. 1990. HMW-2, the Sertoli cell cytoplasmic dynein from rat testis, is a dimer composed of nearly identical subunits. *J. Biol. Chem.* 265:8691–8698.

Ray, S., E. Meyhofer, R. A. Milligan, and J. Howard. 1993. Kinesin follows the microtubule's protofilament axis. *J. Cell Biol.* 121: 1083–1093.

Sale, W. S., and P. Satir. 1977. The termination of the central microtubules from the cilia of tetrahymena pyriformis. *Cell Biol. Int. Rep.* 1:45–49.

Schnapp, B. J., B. Crise, M. P. Sheetz, T. S. Reese, and S. Khan. 1990. Delayed start-up of kinesin-driven microtubule gliding following inhibition by adenosine 5′-[beta,gamma-imido]triphosphate. *Proc. Natl. Acad. Sci. USA.* 87:10053–10057.

Schnapp, B. J., J. Gelles, and M. P. Sheetz. 1988. Nanometer-scale measurements using video light microscopy. *Cell Motil. Cytoskeleton.* 10: 47–53.

Schnapp, B. J., T. S. Reese, and R. Bechtold. 1992. Kinesin is bound with high affinity to squid axon organelles that move to the plus-end of microtubules. *J. Cell Biol.* 119:389–399.

Schroer, T. A. 1992. Motors for fast axonal transport. *Curr. Opin. Neurobiol.* 2:618–621.

Schroer, T. A., E. R. Steuer, and M. P. Sheetz. 1989. Cytoplasmic dynein is a minus end-directed motor for membranous organelles. *Cell.* 56: 937–946.

Song, Y. H., and E. Mandelkow. 1993. Recombinant kinesin motor domain binds to beta-tubulin and decorates microtubules with a B surface lattice. *Proc. Natl. Acad. Sci. USA.* 90:1671–1675.

Steuer, E. R., L. Wordeman, T. A. Schroer, and M. P. Sheetz. 1990. Localization of cytoplasmic dynein to mitotic spindles and kinetochores. *Nature.* 345:266–268.

Svoboda, K., and S. M. Block. 1994. Force and velocity measured for single kinesin molecules. *Cell.* 77:773–784.

Svoboda, K., C. F. Schmidt, B. J. Schnapp, and S. M. Block. 1993. Direct observation of kinesin stepping by optical trapping interferometry. *Nature.* 365:721–727.

Vale, R. D., B. J. Schnapp, T. S. Reese, and M. P. Sheetz. 1985. Organelle, bead, and microtubule translocations promoted by soluble factors from the squid giant axon. *Cell.* 40:559–569.

Vale, R. D., D. R. Soll, and I. R. Gibbons. 1989. One-dimensional diffusion of microtubules bound to flagellar dynein. *Cell.* 59:915–925.

Vale, R. D., and Y. Y. Toyoshima. 1988. Rotation and translocation of microtubules in vitro induced by dyneins from tetrahymena cilia. *Cell.* 52:459–469.

Vallee, R. B., J. S. Wall, B. M. Paschal, and H. S. Shpetner. 1988. Microtubule-associated protein 1C from brain is a two-headed cytosolic dynein. *Nature.* 332:561–563.

Walker, R. A., and M. P. Sheetz. 1993. Cytoplasmic microtubule-associated motors. *Annu. Rev. Biochem.* 62:429–451.

Williams, R. C., and J. C. Lee. 1982. Preparation of tubulin from brain. *Methods Enzymol.* 85:376–385.

Yang, J. T., W. M. Saxton, R. J. Stewart, E. C. Raff, and L. S. Goldstein. 1990. Evidence that the head of kinesin is sufficient for force generation and motility in vitro. *Science.* 249:42–47.